
FreeMatch: Self-adaptive Thresholding for Semi-supervised Learning

Yidong Wang^{1*}, Hao Chen^{2*}, Qiang Heng³, Wenxin Hou⁴, Yue Fan⁵,
 Zhen Wu⁶, Jindong Wang^{7†}, Marios Savvides², Takahiro Shinozaki¹,
 Bhiksha Raj², Bernt Schiele⁵, Xing Xie⁷

¹Tokyo Institute of Technology, ²Carnegie Mellon University, ³North Carolina State University,
⁴Microsoft STCA, ⁵Max-Planck-Institut für Informatik, ⁶Nanjing University,
⁷Microsoft Research Asia

Abstract

Pseudo labeling and consistency regularization approaches based on confidence thresholding have made great progress in semi-supervised learning (SSL). However, we argue that existing methods might fail to adopt suitable thresholds since they either use a pre-defined / fixed threshold or an ad-hoc threshold adjusting scheme, resulting in inferior performance and slow convergence. We first analyze a motivating example to achieve some intuitions on the relationship between the desirable threshold and model’s learning status. Based on the analysis, we hence propose *FreeMatch* to define and adjust the confidence threshold in a self-adaptive manner according to the model’s learning status. We further introduce a self-adaptive class fairness regularization penalty that encourages the model to produce diverse predictions during the early stages of training. Extensive experimental results indicate the superiority of FreeMatch especially when the labeled data are extremely rare. FreeMatch achieves **5.78%**, **13.59%**, and **1.28%** error rate reduction over the latest state-of-the-art method FlexMatch on CIFAR-10 with 1 label per class, STL-10 with 4 labels per class, and ImageNet with 100 labels per class, respectively.

1 Introduction

Despite the success of deep learning in various fields [1, 2, 3], its superior performance heavily relies on supervised training with sufficient labeled data. However, a large amount of labeled data are usually laborious and expensive to obtain. To alleviate the reliance on labeled data, semi-supervised learning (SSL) [4, 5, 6, 7, 8, 9, 10] is developed to improve the model’s generalization performance by exploiting a massive amount of unlabeled data. Pseudo labeling [11, 12, 13, 14] and consistency regularization [15, 16, 17] are two popular paradigms designed for modern SSL. Recently, the combinations of these two paradigms have shown promising results [18, 6, 19, 20, 21]. The key idea is that the model should produce similar predictions or the same pseudo labels for the same unlabeled data under different perturbations following the smoothness and low-density assumptions in SSL [22].

However, a limitation of these methods is that they either need a *fixed threshold* [18, 6, 21] or an *ad-hoc threshold adjusting scheme* [20] to compute the loss with only confident unlabeled samples. Specifically, UDA [18] and FixMatch [6] retain a fixed high threshold to ensure the quality of useful pseudo labels. However, one fixed high threshold for all unlabeled data could lead to low data utilization in the early training stages and ignore the different learning difficulties of different classes.

*Equal contribution. Work done when Yidong Wang was an intern at Microsoft Research Asia.

†Correspondence to: jindwang@microsoft.com

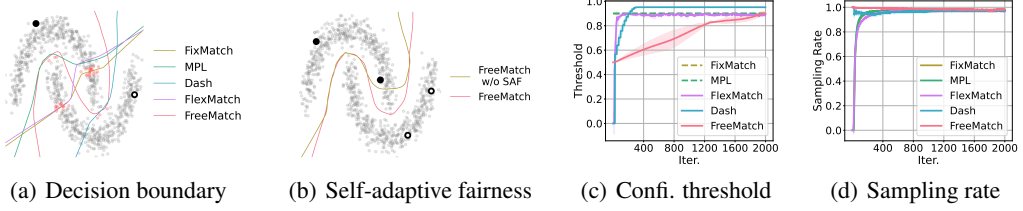


Figure 1: Demonstration of how FreeMatch works on the “two-moon” dataset. We generate only two labeled data points (one label per each class, denoted by black dot and round circle) and 1,000 unlabeled data points (in gray) in 2-D space. We train a 3-layer MLP with 64 neurons in each layer and ReLU activation for 2,000 iterations. The red samples indicate the different samples whose confidence values are above the threshold of FreeMatch but below that of FixMatch. (a) Decision boundary of FreeMatch and other SSL methods. (b) Decision boundary improvement of self-adaptive fairness (SAF) on two labeled samples per class. (c) Class-average confidence threshold. (d) Class-average sampling rate of FreeMatch during training. The sampling rate is computed on unlabeled data as $\sum_b^{N_U} \mathbb{1}(\max(q_b) > \tau) / N_U$. We run the experiments for 5 times to compute the error bars.

Dash [20] proposes to gradually grow the fixed *global* (dataset-specific) threshold as the training progresses. Although the utilization of unlabeled data is improved, their ad-hoc threshold adjusting scheme is arbitrarily controlled by hyper-parameters and thus disconnected from model’s learning process. FlexMatch [21] demonstrates that different classes should have different *local* (class-specific) thresholds based on the numbers of clean unlabeled data whose confidence is higher than a pre-defined global threshold. While the local thresholds take the learning difficulties of different classes into account, they are still mapped from a pre-defined fixed global threshold. In a nutshell, these methods, considering either global or local thresholds alone, might be incapable or insufficient in terms of adjusting thresholds according to the model’s actual learning progress, therefore impeding the training, especially when labeled data is too scarce to provide adequate supervision.

For example, as shown in Figure 1(a), on the “two-moon” dataset with only 1 labeled sample for each class, the decision boundaries obtained by previous methods fail in the low-density assumption. Then, two questions naturally arise: 1) *Is it necessary to determine the threshold based on the model learning status?* and 2) *How to adaptively adjust the threshold for best training efficiency?*

In this paper, we first use a motivating example to demonstrate that different datasets and classes should determine their global (dataset-specific) and local (class-specific) thresholds based on the model’s learning status. Intuitively, we need a low global threshold to utilize more unlabeled data and speed up convergence at early training stages when the model is not very confident. As the prediction confidence increases, a higher global threshold is necessary to filter out wrong pseudo labels to alleviate the confirmation bias [23]. Besides, a local threshold should be defined on each class based on the model’s confidence about its predictions. The “two-moon” example in Figure 1(a) illustrates that the decision boundary is the most reasonable when we adjust the thresholds based on the model’s confidence on unlabeled data.

We then propose *FreeMatch* to adjust the thresholds in a self-adaptive manner according to the model predictions that reflect the learning status of each class [24]. Specifically, FreeMatch uses the self-adaptive thresholding (SAT) technique to estimate both the global (dataset-specific) and local thresholds (class-specific) via the exponential moving average (EMA) of the unlabeled data confidence. To handle barely supervised settings [6] more effectively, we further propose a class fairness objective to encourage the model to produce fair (i.e., diverse) predictions among all classes (as shown in Figure 1(b)). The overall training objective of FreeMatch maximizes the mutual information between model’s input and output [25], producing confident and diverse predictions on unlabeled data. Experimental results on SSL benchmarks validate its effectiveness over other state-of-the-art methods. To conclude, our contributions are:

- Using a motivating example, we discuss why the thresholds should reflect the model’s learning status and provide some intuitions for designing a threshold-adjusting scheme.
- We propose FreeMatch, which consists of Self-Adaptive Thresholding (SAT), a threshold-adjusting scheme that is free of setting thresholds manually and a self-adaptive class

fairness regularization penalty (SAF), which encourages the model to produce more diverse predictions.

- Extensive results demonstrate that FreeMatch achieves significantly superior results on various standard SSL benchmarks, especially when the number of labels is very limited (e.g, an error reduction of **5.78%** on CIFAR-10 with 1 labeled sample per class).

2 A Motivating Example

In this section, we introduce a binary classification example to motivate our threshold-adjusting scheme. Despite the simplification of the actual model and training process, the analysis leads to some interesting implications and provides insight into how the thresholds should be set.

We aim to demonstrate the necessity of the self-adaptability and increased granularity in confidence thresholding for SSL. Inspired by [26], we consider a binary classification problem where the true distribution is an even mixture of two Gaussians (i.e., the label Y is equally likely to be positive (+1) or negative (-1)). The input X has the following conditional distribution:

$$\begin{aligned} X | Y = -1 &\sim \mathcal{N}(\mu_1, \sigma_1^2), \\ X | Y = +1 &\sim \mathcal{N}(\mu_2, \sigma_2^2). \end{aligned} \quad (1)$$

We assume $\mu_2 > \mu_1$ without loss of generality. Suppose that our classifier outputs confidence score:

$$s(x) = \frac{1}{1 + e^{-\beta(x - \frac{\mu_1 + \mu_2}{2})}}, \quad (2)$$

where β is a positive parameter that reflects the model learning status and it is expected to gradually grow during training as the model becomes more confident. Note that $\frac{\mu_1 + \mu_2}{2}$ is in fact the Bayes' optimal linear decision boundary. We consider the scenario where a fixed threshold $\tau \in (\frac{1}{2}, 1)$ is used to generate pseudo labels. A sample x is assigned pseudo label +1 if $s(x) > \tau$ and assigned pseudo label -1 if $s(x) < 1 - \tau$. The pseudo label is 0 (masked) if $1 - \tau \leq s(x) \leq \tau$.

Theorem 2.1. *For a binary classification problem as mentioned above, the pseudo label Y_p has the following probability distribution:*

$$\begin{aligned} P(Y_p = 1) &= \frac{1}{2} \Phi\left(\frac{\frac{\mu_2 - \mu_1}{2} - \frac{1}{\beta} \log(\frac{\tau}{1-\tau})}{\sigma_2}\right) + \frac{1}{2} \Phi\left(\frac{\frac{\mu_1 - \mu_2}{2} - \frac{1}{\beta} \log(\frac{\tau}{1-\tau})}{\sigma_1}\right), \\ P(Y_p = -1) &= \frac{1}{2} \Phi\left(\frac{\frac{\mu_2 - \mu_1}{2} - \frac{1}{\beta} \log(\frac{\tau}{1-\tau})}{\sigma_1}\right) + \frac{1}{2} \Phi\left(\frac{\frac{\mu_1 - \mu_2}{2} - \frac{1}{\beta} \log(\frac{\tau}{1-\tau})}{\sigma_2}\right), \\ P(Y_p = 0) &= 1 - P(Y_p = 1) - P(Y_p = -1), \end{aligned} \quad (3)$$

where Φ is the cumulative distribution function of a standard normal distribution. Moreover, $P(Y_p = 0)$ increases as $\mu_2 - \mu_1$ gets smaller.

The proof is offered in Appendix A. Theorem 2.1 has the following implications or interpretations:

- Trivially, unlabeled data utilization (sampling rate) $1 - P(Y_p = 0)$ is directly controlled by threshold τ . As the confidence threshold τ gets larger, the unlabeled data utilization gets lower. At early training stages, adopting a high threshold may lead to low sampling rate and slow convergence since β is still small.
- More interestingly, $P(Y_p = 1) \neq P(Y_p = -1)$ if $\sigma_1 \neq \sigma_2$. In fact, the larger τ is, the more imbalanced the pseudo labels are. This is potentially undesirable in the sense that we aim to tackle a balanced classification problem. Imbalanced pseudo labels may distort the decision boundary and lead to the so-called pseudo label bias. An easy remedy for this is to use class-specific thresholds τ_2 and $1 - \tau_1$ to assign pseudo labels.
- The sampling rate $1 - P(Y_p = 0)$ decreases as $\mu_2 - \mu_1$ gets smaller. In other words, the more similar the two classes are, the more likely an unlabeled sample will be masked. As the two classes get more similar, there would be more samples mixed in feature space where the model is less confident about its predictions, thus a moderate threshold is needed to balance the sampling rate. Otherwise we may not have enough samples to train the model to classify the already difficult-to-classify classes.

The intuitions provided by Theorem 2.1 is that at the early training stages, τ should be low to encourage diverse pseudo labels, improve unlabeled data utilization and fasten convergence. However, as training continues and β grows larger, a consistently low threshold will lead to unacceptable confirmation bias. Ideally, the threshold τ should increase along with β to maintain a stable sampling rate throughout. Since different classes have different levels of intra-class diversity (different σ) and some classes are harder to classify than others ($\mu_2 - \mu_1$ being small), a fine-grained *class-specific* threshold is desirable to encourage fair assignment of pseudo labels to different classes. The challenge is how to design a threshold adjusting scheme that takes all implications into account, which is the main contribution of this paper. We demonstrate our algorithm by plotting the average threshold trend and marginal pseudo label probability (i.e. sampling rate) during training in Figure 1(c) and 1(d). To sum up, we should determine global (dataset-specific) and local (class-specific) thresholds by estimating the learning status via predictions from the model. We detail our method in the following.

3 Preliminaries

In SSL, the training data consists of labeled and unlabeled data. Let $\mathcal{D}_L = \{(x_b, y_b) : b \in [N_L]\}$ and $\mathcal{D}_U = \{u_b : b \in [N_U]\}$ ³ be the labeled and unlabeled data, where N_L and N_U is their number of samples, respectively. The supervised loss for labeled data is:

$$\mathcal{L}_s = \frac{1}{B} \sum_{b=1}^B \mathcal{H}(y_b, p_m(y|\omega(x_b))), \quad (4)$$

where B is the batch size, $\mathcal{H}(\cdot, \cdot)$ refers to cross-entropy loss, $\omega(\cdot)$ means the stochastic data augmentation function, and $p_m(\cdot)$ is the output probability from the model.

An intuitive approach to leverage unlabeled data is to maximize the mutual information between the model’s input and output on unlabeled data [25]:

$$\mathcal{I}(y, x) = H(\mathbb{E}_u [p_m(y|u)]) - \mathbb{E}_u [H(p_m(y|u))], \quad (5)$$

where \mathbb{E}_u is the expectation over \mathcal{D}_U and $H(\cdot)$ denotes entropy. The first term corresponds to fairness on each class as mentioned in [25] and the second term denotes entropy minimization [27] which makes the unlabeled data decisiveness and model’s decision boundary lie in low-density regions [22].

In this work, we focus on pseudo labeling using cross-entropy loss with confidence threshold for entropy minimization. We also adopt the “Weak and Strong Augmentation” strategy introduced by UDA [18]. Formally, the unsupervised training objective for unlabeled data is:

$$\mathcal{L}_u = \frac{1}{\mu B} \sum_{b=1}^{\mu B} \mathbb{1}(\max(q_b) > \tau) \cdot \mathcal{H}(\hat{q}_b, Q_b). \quad (6)$$

We use q_b and Q_b to denote abbreviation of $p_m(y|\omega(u_b))$ and $p_m(y|\Omega(u_b))$, respectively. \hat{q}_b is the hard “one-hot” label converted from q_b , μ is the ratio of unlabeled data batch size to labeled data batch size, and $\mathbb{1}(\cdot > \tau)$ is the indicator function for confidence-based thresholding with τ being the threshold. The weak augmentation (i.e., random crop and flip) and strong augmentation (i.e., RandAugment [28]) is represented by $\omega(\cdot)$ and $\Omega(\cdot)$ respectively.

The fairness objective \mathcal{L}_f is used to encourage the model to predict each class at the same frequency, which is usually in the form of $\mathcal{L}_f = \mathbf{U} \log \mathbb{E}_{\mu B} [q_b]$ [29], where \mathbf{U} stands for a uniform prior distribution. One may notice that using a uniform prior not only prevents the generalization to non-uniform data distribution but also ignores the fact that the underlying pseudo label distribution for a mini-batch may be imbalanced due to the sampling mechanism. The uniformity across a batch is essential for fair utilization of samples with per-class threshold, especially during early-training.

4 FreeMatch

4.1 Self-Adaptive Thresholding

We advocate that the key to determining thresholds for SSL is that thresholds should reflect the learning status. The learning effect can be estimated by the prediction confidence of a well-calibrated

³ $[N] := \{1, 2, \dots, N\}$.

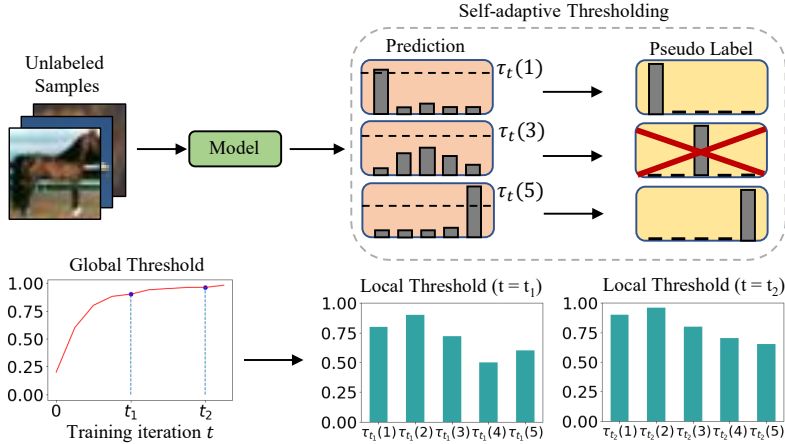


Figure 2: Illustration of Self-Adaptive Thresholding (SAT). Instead of using fixed (FixMatch [6]) or partially flexible global (Dash [20]) / local (FlexMatch [21]) thresholding to filter unlabeled samples, FreeMatch adopts both global and local self-adaptive thresholds computed from the EMA of prediction statistics from unlabeled samples. Filtered (masked) samples are marked with red X.

model [24]. Hence, we propose *self-adaptive thresholding* (SAT) that automatically defines and adaptively adjusts the confidence threshold for each class by leveraging the model predictions during training. SAT first estimates a global threshold as the EMA of the confidence from the model. Then, SAT modulates the global threshold via the local class-specific thresholds estimated as the EMA of the probability for each class from the model. When training starts, the threshold is low to accept more possibly correct samples into training. As the model becomes more confident, the threshold adaptively increases to filter out possibly incorrect samples to reduce the confirmation bias. Thus, as shown in Figure 2, we define SAT as $\tau_t(c)$ indicating the threshold for class c at the t -th iteration.

Self-adaptive Global Threshold We design the global threshold based on the following two principles. First, the global threshold in SAT should be related to the model’s confidence on unlabeled data, reflecting the overall learning status. Moreover, the global threshold should stably increase during training to ensure incorrect pseudo labels are discarded. We set the global threshold τ_t as average confidence from the model on unlabeled data, where t represents the t -th time step (iteration). However, it would be time-consuming to compute the confidence for all unlabeled data at every time step or even every training epoch due to its large volume. Instead, we estimate the global confidence as the exponential moving average (EMA) of the confidence at each training time step. We initialize τ_t as $\frac{1}{C}$ where C indicates the number of classes. The global threshold τ_t is defined and adjusted as:

$$\tau_t = \begin{cases} \frac{1}{C}, & \text{if } t = 0, \\ \lambda \tau_{t-1} + (1 - \lambda) \frac{1}{\mu B} \sum_{b=1}^{\mu B} \max(q_b), & \text{otherwise,} \end{cases} \quad (7)$$

where $\lambda \in (0, 1)$ is the momentum decay of EMA.

Self-adaptive Local Threshold The local threshold aims to modulate the global threshold in a class-specific fashion to account for the intra-class diversity and the possible class adjacency. We compute the expectation of the model’s predictions on each class c to estimate the class-specific learning status:

$$\tilde{p}_t(c) = \begin{cases} \frac{1}{C}, & \text{if } t = 0, \\ \lambda \tilde{p}_{t-1}(c) + (1 - \lambda) \frac{1}{\mu B} \sum_{b=1}^{\mu B} q_b(c), & \text{otherwise,} \end{cases} \quad (8)$$

where $\tilde{p}_t = [\tilde{p}_t(1), \tilde{p}_t(2), \dots, \tilde{p}_t(C)]$ is the list containing all $\tilde{p}_t(c)$. Integrating the global and local thresholds, we obtain the final self-adaptive threshold $\tau_t(c)$ as:

$$\tau_t(c) = \text{MaxNorm}(\tilde{p}_t(c)) \cdot \tau_t = \frac{\tilde{p}_t(c)}{\max\{\tilde{p}_t(c) : c \in [C]\}} \cdot \tau_t, \quad (9)$$

where MaxNorm is the Maximum Normalization (i.e., $x' = \frac{x}{\max(x)}$). Finally, the unsupervised training objective \mathcal{L}_u at the t -th iteration is:

$$\mathcal{L}_u = \frac{1}{\mu B} \sum_{b=1}^{\mu B} \mathbb{1}(\max(q_b) > \tau_t(\arg \max(q_b)) \cdot \mathcal{H}(\hat{q}_b, Q_b)). \quad (10)$$

4.2 Self-Adaptive Fairness

We include the class fairness objective as mentioned in Section 3 into FreeMatch to encourage the model to make diverse predictions for each class and thus produce a meaningful self-adaptive threshold, especially under the settings where labeled data are rare. Instead of using a uniform prior as in [23], we use the EMA of model predictions \tilde{p}_t from Eq. (8) as an estimate of the expectation of prediction distribution over unlabeled data. We optimize the cross-entropy of \tilde{p}_t and $\bar{p} = \mathbb{E}_{\mu B}[p_m(y|\Omega(u_b))]$ over mini-batch as an estimate of $H(\mathbb{E}_u[p_m(y|u)])$. Considering that the underlying pseudo label distribution may not be uniform, we propose to modulate the fairness objective in a self-adaptive way, i.e., normalizing the expectation of probability by the histogram distribution of pseudo labels to counter the negative effect of imbalance as:

$$\begin{aligned} \bar{p} &= \frac{1}{\mu B} \sum_{b=1}^{\mu B} \mathbb{1}(\max(q_b) \geq \tau_t(\arg \max(q_b)) Q_b), \\ \bar{h} &= \text{Hist}_{\mu B} \left(\mathbb{1}(\max(q_b) \geq \tau_t(\arg \max(q_b)) \hat{Q}_b) \right). \end{aligned} \quad (11)$$

Similar to \tilde{p}_t , we compute \tilde{h}_t as:

$$\tilde{h}_t = \lambda \tilde{h}_{t-1} + (1 - \lambda) \text{Hist}_{\mu B}(\hat{q}_b). \quad (12)$$

The self-adaptive fairness (SAF) \mathcal{L}_f at the t -th iteration is formulated as:

$$\mathcal{L}_f = -\mathcal{H} \left(\text{SumNorm} \left(\frac{\tilde{p}_t}{\tilde{h}_t} \right), \text{SumNorm} \left(\frac{\bar{p}}{\bar{h}} \right) \right), \quad (13)$$

where $\text{SumNorm} = \frac{(\cdot)}{\sum(\cdot)}$. SAF encourages the expectation of the output probability for each mini-batch to be close to a marginal class distribution of the model, after normalized by histogram distribution. It helps the model produce diverse predictions especially for barely supervised settings [6], and therefore converges faster and generalizes better. This is also illustrated in Figure 1(b).

The overall objective for FreeMatch at t -th iteration is:

$$\mathcal{L} = \mathcal{L}_s + w_u \mathcal{L}_u + w_f \mathcal{L}_f, \quad (14)$$

where w_u and w_f represents the loss weight for \mathcal{L}_u and \mathcal{L}_f respectively. With \mathcal{L}_u and \mathcal{L}_f , FreeMatch maximizes the mutual information between its outputs and inputs. We present the procedure of FreeMatch in Algorithm 1 of Appendix.

5 Experiments

5.1 Setup

We evaluate FreeMatch on common benchmarks: CIFAR-10/100 [30], SVHN [31], STL-10 [32] and ImageNet [33]. Following previous work [6, 20, 21, 34], we conduct experiments with varying amounts of labeled data. In addition to the commonly-chosen labeled amounts, following [6], we further include the most challenging case of CIFAR-10: each class has only *one* labeled sample.

For fair comparison, we train and evaluate all methods using the unified codebase TorchSSL [21] with the same backbones and hyperparameters. Concretely, we use Wide ResNet-28-2 [35] for CIFAR-10, Wide ResNet-28-8 for CIFAR-100, Wide ResNet-37-2 [36] for STL-10, and ResNet-50 [1] for ImageNet. We use SGD with a momentum of 0.9 as optimizer. The initial learning rate is 0.03 with a cosine learning rate decay schedule as $\eta = \eta_0 \cos(\frac{7\pi k}{16K})$, where η_0 is the initial learning rate, $k(K)$ is

Table 1: Error rates on CIFAR-10/100, SVHN, and STL-10 datasets. The fully-supervised results of STL-10 are unavailable since we do not have label information for its unlabeled data. **Bold** indicates the best result and underline indicates the second-best result.

Dataset	CIFAR-10				CIFAR-100			SVHN			STL-10	
	10	40	250	4000	400	2500	10000	40	250	1000	40	1000
II Model [37]	79.18 \pm 1.11	74.34 \pm 1.76	46.24 \pm 1.29	13.13 \pm 0.59	86.96 \pm 0.80	58.80 \pm 0.66	36.65 \pm 0.00	67.48 \pm 0.95	13.30 \pm 1.12	7.16 \pm 0.11	74.31 \pm 0.85	32.78 \pm 0.40
Pseudo Label [11]	80.21 \pm 0.55	74.61 \pm 0.26	46.49 \pm 2.20	15.08 \pm 0.16	87.45 \pm 0.85	57.74 \pm 0.28	36.55 \pm 0.24	64.61 \pm 5.6	15.59 \pm 0.95	9.40 \pm 0.32	74.68 \pm 0.99	32.64 \pm 0.71
VAT [39]	79.81 \pm 1.17	74.66 \pm 2.12	41.03 \pm 1.79	10.51 \pm 0.12	85.20 \pm 1.40	46.84 \pm 0.79	32.14 \pm 0.19	74.75 \pm 3.38	4.33 \pm 0.12	4.11 \pm 0.20	74.74 \pm 0.38	37.95 \pm 1.12
Mean Teacher [38]	76.37 \pm 0.44	70.09 \pm 1.60	37.46 \pm 3.30	8.10 \pm 0.21	81.11 \pm 1.44	45.17 \pm 1.06	31.75 \pm 0.23	36.09 \pm 3.98	3.45 \pm 0.08	3.27 \pm 0.08	71.72 \pm 1.45	33.90 \pm 1.37
MixMatch [40]	65.76 \pm 7.06	36.19 \pm 6.48	13.63 \pm 0.59	6.66 \pm 0.26	67.59 \pm 6.66	39.76 \pm 0.48	27.78 \pm 0.29	30.60 \pm 8.39	4.56 \pm 0.32	3.69 \pm 0.37	54.93 \pm 0.96	21.70 \pm 0.68
ReMixMatch [41]	20.77 \pm 7.48	9.88 \pm 1.03	6.30 \pm 0.05	4.84 \pm 0.01	42.75 \pm 1.05	26.03 \pm 0.35	20.02 \pm 0.27	24.04 \pm 9.13	6.36 \pm 0.22	5.16 \pm 0.31	32.12 \pm 6.24	6.74 \pm 0.14
UDA [18]	34.53 \pm 10.69	10.62 \pm 3.75	5.16 \pm 0.06	4.29 \pm 0.07	46.39 \pm 1.59	27.73 \pm 0.21	22.49 \pm 0.23	5.12 \pm 4.27	1.92 \pm 0.05	1.89 \pm 0.01	37.42 \pm 8.44	6.64 \pm 0.17
FixMatch [6]	24.79 \pm 7.65	7.47 \pm 0.28	4.86 \pm 0.05	4.21 \pm 0.08	46.42 \pm 0.82	28.03 \pm 0.16	22.20 \pm 0.12	3.81 \pm 1.18	2.02 \pm 0.04	1.96 \pm 0.03	35.97 \pm 4.14	6.25 \pm 0.33
Dash [20]	27.28 \pm 14.09	8.93 \pm 3.11	5.16 \pm 0.23	4.36 \pm 0.11	44.82 \pm 0.96	27.15 \pm 0.22	21.88 \pm 0.07	2.19 \pm 0.18	2.04 \pm 0.02	1.97 \pm 0.01	34.52 \pm 4.30	6.39 \pm 0.56
MPL [19]	23.55 \pm 6.01	6.62 \pm 0.91	5.76 \pm 0.24	4.55 \pm 0.04	46.26 \pm 1.84	27.71 \pm 0.19	21.74 \pm 0.09	9.33 \pm 8.02	2.29 \pm 0.02	2.28 \pm 0.02	35.76 \pm 4.83	6.66 \pm 0.00
FlexMatch [21]	13.85 \pm 12.04	4.97 \pm 0.06	4.98 \pm 0.09	4.19 \pm 0.01	39.94 \pm 1.62	26.49 \pm 0.20	21.90 \pm 0.15	8.19 \pm 3.20	6.59 \pm 2.29	6.72 \pm 0.30	29.15 \pm 4.16	5.77 \pm 0.18
FreeMatch	8.07 \pm 4.24	4.90 \pm 0.04	4.88 \pm 0.18	4.10 \pm 0.02	37.98 \pm 0.42	26.47 \pm 0.20	<u>21.68</u> \pm 0.03	1.97 \pm 0.02	<u>1.97</u> \pm 0.01	<u>1.96</u> \pm 0.03	15.56 \pm 0.55	5.63 \pm 0.15
Fully-Supervised			4.62 \pm 0.05			19.30 \pm 0.09		2.13 \pm 0.01			-	

the current (total) training step and we set $K = 2^{20}$ for all datasets. At the testing phase, we use an exponential moving average with the momentum of 0.999 of the training model to conduct inference for all algorithms. The batch size of labeled data is 64 except for ImageNet where we set 128. We use the same weight decay value, pre-defined threshold τ , unlabeled batch ratio μ and loss weights introduced for Pseudo-Label [11], II model [37], Mean Teacher [38], VAT [39], MixMatch [40], ReMixMatch [41], UDA [18], FixMatch [6], and FlexMatch [21].

We implement MPL based on UDA as in [19], where we set temperature as 0.8 and w_u as 10. We do not fine-tune MPL on labeled data as in [19] since we find fine-tuning will make the model overfit the labeled data especially with very few of them. For Dash, we use the same parameters as in [20] except we warm-up on labeled data for 2 epochs since too much warm-up will lead to the overfitting (i.e. 2,048 training iterations). For FreeMatch, we set $w_u = 1$ for all experiments. Besides, we set $w_f = 0.01$ for CIFAR-10 with 10 labels, CIFAR-100 with 400 labels, STL-10 with 40 labels, ImageNet with 100k labels, and all experiments for SVHN. For other settings, we use $w_f = 0.05$. For SVHN, we find that using a low threshold at early training stage impedes the model to cluster the unlabeled data, thus we adopt two training techniques for SVHN: (1) warm-up the model on only labeled data for 2 epochs as Dash; and (2) restrict the SAT within the range $[0.9, 0.95]$. The detailed hyperparameters are introduced in Appendix C. We train each algorithm 3 times using different random seeds. Following [21], we report the best error rates of all checkpoints.

5.2 Quantitative Results

The Top-1 classification error rates of CIFAR-10/100, SVHN, and STL-10 are reported in Table 1. The results on ImageNet with 100 labels per class are in Table 2. We also provide detailed results on precision, recall, F1 score, and confusion matrix in Appendix D.2. These quantitative results demonstrate that FreeMatch achieves the best performance on CIFAR-10, STL-10, and ImageNet datasets, and it produces very close results on SVHN to the best competitor. On CIFAR-100, FreeMatch is better than ReMixMatch when there are 400 labels. The good performances of ReMixMatch on CIFAR-100 (2500) and CIFAR-100 (10000) are probably brought by the mix up [42] technique and the self-supervised learning part. On ImageNet with 100k labels, FreeMatch significantly outperforms the latest counterpart FlexMatch by **1.28%**⁴. We also notice that FreeMatch exhibits fast computation in ImageNet from Table 2. Note that FlexMatch is much slower than FixMatch and FreeMatch because it needs to maintain a list that records whether each sample is clean, which needs heavy indexing computation budget on large datasets. Noteworthy is that, FreeMatch consistently outperforms other methods by a large margin on settings with *extremely limited labeled data*: **5.78%** on CIFAR-10 with 10 labels, **1.96%** on CIFAR-100 with 400 labels, and surprisingly **13.59%** on STL-10 with 40 labels. STL-10 is a more realistic and challenging dataset compared to others, which consists of a large unlabeled set of 100k images. The significant improvements demonstrate the capability and potential of FreeMatch to be deployed in real-world applications.

Table 2: Error rates and runtime on ImageNet with 100 labels per class.

	Top-1	Top-5	Runtime (sec./iter.)
FixMatch	43.66	21.80	0.4
FlexMatch	41.85	19.48	0.6
FreeMatch	40.57	18.77	0.4

⁴Following [21], we train ImageNet for 2^{20} iterations like other datasets for a fair comparison. We use 4 Tesla V100 GPUs on ImageNet.

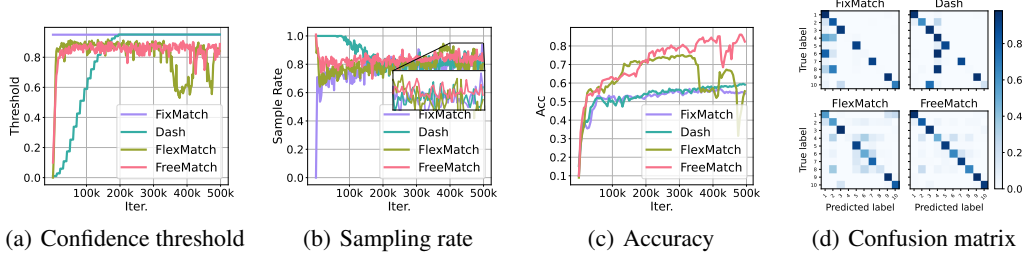


Figure 3: Demonstration of how FreeMatch works in STL-10 with 40 labels, compared to previous methods. (a) Class-average confidence threshold; (b) class-average sampling rate; (c) convergence speed in terms of accuracy; (d) confusion matrix, where the fading color of diagonal elements refers to the disparity of the accuracy.

5.3 Qualitative Analysis

We present some qualitative analysis: Why and how does FreeMatch work? What other benefits does it bring? We evaluate the class average threshold and average sampling rate on STL-10 (40) (i.e., 40 labeled samples on STL-10) of FreeMatch to demonstrate how it works aligning with our theoretical analysis. We record the threshold and compute the sampling rate for each batch during training.

The sampling rate is calculated on unlabeled data as $\frac{\sum_b^{\mu B} \mathbb{1}(\max(q_b) > \tau_t(\arg \max(q_b)))}{\mu B}$. We also plot the convergence speed in terms of accuracy and the confusion matrix to show the proposed component in FreeMatch helps improve performance. From Figure 3(a) and Figure 3(b), one can observe that the threshold and sampling rate change of FreeMatch is mostly consistent with our theoretical analysis. That is, at the early stage of training, the threshold of FreeMatch is relatively lower, compared to FlexMatch and FixMatch, resulting in higher unlabeled data utilization (sampling rate), which fastens the convergence. As the model learns better and becomes more confident, the threshold of FreeMatch increases to a high value to alleviate the confirmation bias, leading to stably high sampling rate. Correspondingly, the accuracy of FreeMatch increases vastly (as shown in Figure 3(c)) and resulting better class-wise accuracy (as shown in Figure 3(d)). Note that Dash fails to learn properly due to the employment of the high sampling rate until 100k iterations.

To further demonstrate the effectiveness of the class-specific threshold in FreeMatch, we present the t-SNE [43] visualization of features of FlexMatch and FreeMatch on STL-10 (40) in Figure 5 of Appendix D.5. We exhibit the corresponding local threshold for each class. Interestingly, FlexMatch has a high threshold, i.e., pre-defined 0.95, for class 0 and class 6, yet their feature variances are very large and are confused with other classes. This means the class-wise thresholds in FlexMatch cannot accurately reflect the learning status. In contrast, FreeMatch clusters most classes better. Besides, for the similar classes 1, 3, 5, 7 that are confused with each other, FreeMatch retains a higher average threshold 0.87 than 0.84 of FlexMatch, enabling to mask more wrong pseudo labels.

5.4 Ablation Study

Self-adaptive Threshold We conduct experiments on the components of SAT in FreeMatch and compare to the components in FlexMatch [21], FixMatch [6], Class-Balanced Self-Training (CBST) [44], and Relative Threshold (RT) in AdaMatch [45]. The ablation is conducted on CIFAR-10 (40 labels). As shown in Table 3, SAT achieves the best performance among all the threshold schemes. Self-adaptive global threshold τ_t and local threshold $\text{MaxNorm}(\tilde{p}_t(c))$ themselves also achieve comparable results, compared to the fixed threshold τ , demonstrating both local and global threshold proposed are good learning effect estimators. When using CPL $\mathcal{M}(\beta(c))$ to adjust τ_t , the result is worse than the fixed threshold and exhibits larger variance, indicating potential instability of CPL. AdaMatch [45] uses the RT, which can be viewed as a global threshold at t -th iteration computed on the predictions of labeled data without EMA, whereas FreeMatch conducts computation of τ_t with EMA on unlabeled data that can better reflect the overall data distribution. For class-wise threshold, CBST [44] maintains a pre-defined sampling rate, which

Table 3: Comparison of different thresholding schemes.

Threshold	CIFAR-10 (40)
τ (FixMatch)	7.47 ± 0.28
$\tau * \mathcal{M}(\beta(c))$ (FlexMatch)	4.97 ± 0.06
$\tau * \text{MaxNorm}(\tilde{p}_t(c))$	5.13 ± 0.03
τ_t (Global)	6.06 ± 0.65
$\tau_t * \mathcal{M}(\beta(c))$	8.40 ± 2.49
CBST	16.65 ± 2.90
RT (AdaMatch)	6.09 ± 0.65
SAT (Global and Local)	4.92 ± 0.04

could be the reason for its bad performance since the sampling rate should be changed during training as we analyzed in Sec. 2. Note that we did not include L_f in this ablation for a fair comparison.

Self-adaptive Fairness As illustrated in Table 4, we also empirically study the effect of SAF on CIFAR-10 (10 labels). We study the original version of fairness objective as in [23]. Based on that, we study the operation of normalization probability by histograms and show that countering the effect of imbalanced underlying distribution indeed helps the model to learn and diverse better. One may notice that adding original fairness regularization alone already helps improve the performance. Whereas adding normalization operation in the log operation hurts the performance, suggesting the underlying batch data are indeed not uniformly distributed. We also evaluate Distribution Alignment (DA) for class fairness proposed in ReMixMatch [41] and AdaMatch [45], which shows inferior results compared to SAF. A possible reason for the bad performance of DA (AdaMatch) is that it only uses labeled batch prediction as the target distribution which cannot reflect the true data distribution especially when labeled data is scarce and changing the target distribution to the ground truth uniform, i.e., DA (ReMixMatch), is better for the case with extremely limited labels.

Table 4: Comparison of different class fairness objectives.

Fairness	CIFAR-10 (10)
w/o fairness	10.37 ± 7.70
$U \log \bar{p}$	9.57 ± 6.67
$U \log \text{SumNorm}(\frac{\bar{p}}{h})$	12.07 ± 5.23
DA (AdaMatch)	32.94 ± 1.83
DA (ReMixMatch)	11.06 ± 8.21
SAF	8.07 ± 4.24

Thresholding EMA Decay and Performance in Imbalanced Settings We validate the effect of EMA decay parameter λ on CIFAR-10 (40) in Table 9 of Appendix D.3, showing that FreeMatch is robust to λ . We further show in Table 10 of Appendix D.4 that FreeMatch outperforms other baselines and can be plugged in the other imbalanced SSL method for better results in imbalanced settings.

6 Related Work

Self-training is widely adopted in SSL [37, 38, 40, 41, 18, 12, 46, 47, 48]. The overall idea is treating the model’s output probabilities as soft labels for unlabeled data. Pseudo labeling is a variant of self-training that converts probabilities to hard labels [11, 6]. Consistency regularization is used to force the predictions on the perturbed versions of unlabeled data to be similar to the pseudo labels [17, 6].

To reduce confirmation bias [23] in self-training, confidence-based thresholding techniques are proposed to ensure the quality of pseudo labels [18, 6, 21, 20], where only the unlabeled data whose confidences are higher than the threshold are retained. UDA [18] and FixMatch [6] keep the fixed pre-defined threshold during training. FlexMatch [21] adjusts the pre-defined threshold in a class-specific fashion according to the per-class learning status estimated by the number of confident unlabeled data. Dash [20] defines a threshold according to the loss on labeled data and adjusts the threshold according to a fixed mechanism. Besides, AdaMatch [45] aims to unify SSL and domain adaptation with the thresholds based on the labeled data batch. It ignores the unlabeled data distribution especially when labeled data is too rare to reflect the unlabeled data distribution. Besides, dynamic thresholding technique has been investigated in other fields such as sentiment analysis [49] and semantic segmentation [50]. In [49], labeled data set is expanded by selecting confident data from unlabeled data via a gradually reduced threshold. In [50], threshold is modified by an extra classifier. Curriculum learning is introduced to adjust the threshold in [51, 21]. Previous methods might fail to choose meaningful thresholds due to ignorance of the relationship between the model learning status and thresholds, while ours can adjust meaningful thresholds according to the learning status.

Except consistency regularization, entropy-based regularization is also used in SSL. Entropy minimization [27] encourages the model to make confident predictions for all samples disregarding the actual class predicted. Maximization of expectation of entropy [29, 23] over all samples is also proposed to induce fairness to the model, enforcing the model to predict each class at the same frequency. But previous ones assume a uniform prior for underlying data distribution and also ignore the batch data distribution. Distribution alignment [41] adjusts the pseudo labels according to labeled data distribution and the EMA of model predictions. The SAF in FreeMatch considers the issue of non-uniform distribution, stabilizing the estimation of SAT especially for early training.

7 Conclusion

In this paper, we proposed FreeMatch, an SSL method which utilizes self-adaptive thresholding and class-fairness regularization. FreeMatch outperforms existing state-of-the-art methods across a variety of SSL benchmarks, especially in the barely-supervised setting. We also used a motivating example analysis to provide some intuitions on how to design the threshold adjusting scheme. We believe that confidence thresholding has even more potential in SSL and we hope that the effectiveness of FreeMatch inspires more research into the optimal way of thresholding. The future work also includes more realistic settings such as imbalanced SSL [52, 53, 54, 55] and open-set SSL [56, 57].

References

- [1] Kaiming He, Xiangyu Zhang, Shaoqing Ren, and Jian Sun. Deep residual learning for image recognition. In *Proceedings of the IEEE conference on computer vision and pattern recognition*, pages 770–778, 2016.
- [2] Ashish Vaswani, Noam Shazeer, Niki Parmar, Jakob Uszkoreit, Llion Jones, Aidan N Gomez, Łukasz Kaiser, and Illia Polosukhin. Attention is all you need. *Advances in neural information processing systems*, 30, 2017.
- [3] Linhao Dong, Shuang Xu, and Bo Xu. Speech-transformer: a no-recurrence sequence-to-sequence model for speech recognition. In *2018 IEEE International Conference on Acoustics, Speech and Signal Processing (ICASSP)*, pages 5884–5888. IEEE, 2018.
- [4] Xiaojin Jerry Zhu. Semi-supervised learning literature survey. 2005.
- [5] Xiaojin Zhu and Andrew B Goldberg. Introduction to semi-supervised learning. *Synthesis lectures on artificial intelligence and machine learning*, 3(1):1–130, 2009.
- [6] Kihyuk Sohn, David Berthelot, Nicholas Carlini, Zizhao Zhang, Han Zhang, Colin A Raf-fel, Ekin Dogus Cubuk, Alexey Kurakin, and Chun-Liang Li. Fixmatch: Simplifying semi-supervised learning with consistency and confidence. *Advances in Neural Information Processing Systems*, 33, 2020.
- [7] Chuck Rosenberg, Martial Hebert, and Henry Schneiderman. Semi-supervised self-training of object detection models. 2005.
- [8] Chen Gong, Dacheng Tao, Stephen J Maybank, Wei Liu, Guoliang Kang, and Jie Yang. Multi-modal curriculum learning for semi-supervised image classification. *IEEE Transactions on Image Processing*, 25(7):3249–3260, 2016.
- [9] Hoel Kervadec, Jose Dolz, Éric Granger, and Ismail Ben Ayed. Curriculum semi-supervised segmentation. In *International Conference on Medical Image Computing and Computer-Assisted Intervention*, pages 568–576. Springer, 2019.
- [10] Zihang Dai, Zhilin Yang, Fan Yang, William W Cohen, and Russ R Salakhutdinov. Good semi-supervised learning that requires a bad gan. *Advances in neural information processing systems*, 30, 2017.
- [11] Dong-Hyun Lee et al. Pseudo-label: The simple and efficient semi-supervised learning method for deep neural networks. In *Workshop on challenges in representation learning, ICML*, volume 3, page 896, 2013.
- [12] Qizhe Xie, Minh-Thang Luong, Eduard Hovy, and Quoc V Le. Self-training with noisy student improves imagenet classification. In *Proceedings of the IEEE/CVF Conference on Computer Vision and Pattern Recognition*, pages 10687–10698, 2020.
- [13] Geoffrey J McLachlan. Iterative reclassification procedure for constructing an asymptotically optimal rule of allocation in discriminant analysis. *Journal of the American Statistical Association*, 70(350):365–369, 1975.
- [14] Mamshad Nayeem Rizve, Kevin Duarte, Yogesh S Rawat, and Mubarak Shah. In defense of pseudo-labeling: An uncertainty-aware pseudo-label selection framework for semi-supervised learning. In *International Conference on Learning Representations*, 2020.
- [15] Philip Bachman, Ouais Alsharif, and Doina Precup. Learning with pseudo-ensembles. *Advances in neural information processing systems*, 27:3365–3373, 2014.

- [16] Laine Samuli and Aila Timo. Temporal ensembling for semi-supervised learning. In *International Conference on Learning Representations (ICLR)*, volume 4, page 6, 2017.
- [17] Mehdi Sajjadi, Mehran Javanmardi, and Tolga Tasdizen. Regularization with stochastic transformations and perturbations for deep semi-supervised learning. *Advances in neural information processing systems*, 29:1163–1171, 2016.
- [18] Qizhe Xie, Zihang Dai, Eduard Hovy, Thang Luong, and Quoc Le. Unsupervised data augmentation for consistency training. *Advances in Neural Information Processing Systems*, 33, 2020.
- [19] Hieu Pham, Zihang Dai, Qizhe Xie, and Quoc V Le. Meta pseudo labels. In *Proceedings of the IEEE/CVF Conference on Computer Vision and Pattern Recognition*, pages 11557–11568, 2021.
- [20] Yi Xu, Lei Shang, Jinxing Ye, Qi Qian, Yu-Feng Li, Baigui Sun, Hao Li, and Rong Jin. Dash: Semi-supervised learning with dynamic thresholding. In *International Conference on Machine Learning*, pages 11525–11536. PMLR, 2021.
- [21] Bowen Zhang, Yidong Wang, Wenxin Hou, Hao Wu, Jindong Wang, Manabu Okumura, and Takahiro Shinohara. Flexmatch: Boosting semi-supervised learning with curriculum pseudo labeling. *Advances in Neural Information Processing Systems*, 34, 2021.
- [22] Olivier Chapelle, Bernhard Schölkopf, and Alexander Zien, editors. *Semi-Supervised Learning*. The MIT Press, 2006.
- [23] Eric Arazo, Diego Ortego, Paul Albert, Noel E O’Connor, and Kevin McGuinness. Pseudo-labeling and confirmation bias in deep semi-supervised learning. In *2020 International Joint Conference on Neural Networks (IJCNN)*, pages 1–8. IEEE, 2020.
- [24] Chuan Guo, Geoff Pleiss, Yu Sun, and Kilian Q Weinberger. On calibration of modern neural networks. In *International Conference on Machine Learning*, pages 1321–1330. PMLR, 2017.
- [25] David MacKay John Bridle, Anthony Heading. Unsupervised classifiers, mutual information and ‘phantom targets’. 1991.
- [26] Yuzhe Yang and Zhi Xu. Rethinking the value of labels for improving class-imbalanced learning. In *NeurIPS*, 2020.
- [27] Yves Grandvalet, Yoshua Bengio, et al. Semi-supervised learning by entropy minimization. volume 367, pages 281–296, 2005.
- [28] Ekin D Cubuk, Barret Zoph, Jonathon Shlens, and Quoc V Le. Randaugment: Practical automated data augmentation with a reduced search space. In *Proceedings of the IEEE/CVF Conference on Computer Vision and Pattern Recognition Workshops*, pages 702–703, 2020.
- [29] Ryan Gomes Andreas Krause, Pietro Perona. Discriminative clustering by regularized information maximization. In *Advances in neural information processing systems*, 2010.
- [30] Alex Krizhevsky et al. Learning multiple layers of features from tiny images. 2009.
- [31] Yuval Netzer, Tao Wang, Adam Coates, Alessandro Bissacco, Bo Wu, and Andrew Y Ng. Reading digits in natural images with unsupervised feature learning. 2011.
- [32] Adam Coates, Andrew Ng, and Honglak Lee. An analysis of single-layer networks in unsupervised feature learning. In *Proceedings of the fourteenth international conference on artificial intelligence and statistics*, pages 215–223. JMLR Workshop and Conference Proceedings, 2011.
- [33] Jia Deng, Wei Dong, Richard Socher, Li-Jia Li, Kai Li, and Li Fei-Fei. Imagenet: A large-scale hierarchical image database. In *2009 IEEE conference on computer vision and pattern recognition*, pages 248–255. Ieee, 2009.
- [34] Avital Oliver, Augustus Odena, Colin A Raffel, Ekin Dogus Cubuk, and Ian Goodfellow. Realistic evaluation of deep semi-supervised learning algorithms. *Advances in neural information processing systems*, 31, 2018.
- [35] Sergey Zagoruyko and Nikos Komodakis. Wide residual networks. In *British Machine Vision Conference 2016*. British Machine Vision Association, 2016.
- [36] Tianyi Zhou, Shengjie Wang, and Jeff Bilmes. Time-consistent self-supervision for semi-supervised learning. In *International Conference on Machine Learning*, pages 11523–11533. PMLR, 2020.

- [37] Antti Rasmus, Mathias Berglund, Mikko Honkala, Harri Valpola, and Tapani Raiko. Semi-supervised learning with ladder networks. *Advances in Neural Information Processing Systems*, 28:3546–3554, 2015.
- [38] Antti Tarvainen and Harri Valpola. Mean teachers are better role models: Weight-averaged consistency targets improve semi-supervised deep learning results. In *Proceedings of the 31st International Conference on Neural Information Processing Systems*, pages 1195–1204, 2017.
- [39] Takeru Miyato, Shin-ichi Maeda, Masanori Koyama, and Shin Ishii. Virtual adversarial training: a regularization method for supervised and semi-supervised learning. *IEEE transactions on pattern analysis and machine intelligence*, 41(8):1979–1993, 2018.
- [40] David Berthelot, Nicholas Carlini, Ian Goodfellow, Nicolas Papernot, Avital Oliver, and Colin A Raffel. Mixmatch: A holistic approach to semi-supervised learning. *Advances in Neural Information Processing Systems*, 32, 2019.
- [41] David Berthelot, Nicholas Carlini, Ekin D Cubuk, Alex Kurakin, Kihyuk Sohn, Han Zhang, and Colin Raffel. Remixmatch: Semi-supervised learning with distribution matching and augmentation anchoring. In *International Conference on Learning Representations*, 2019.
- [42] Hongyi Zhang, Moustapha Cisse, Yann N Dauphin, and David Lopez-Paz. mixup: Beyond empirical risk minimization. *arXiv preprint arXiv:1710.09412*, 2017.
- [43] Laurens Van der Maaten and Geoffrey Hinton. Visualizing data using t-sne. *Journal of machine learning research*, 9(11), 2008.
- [44] Yang Zou, Zhiding Yu, BVK Kumar, and Jinsong Wang. Unsupervised domain adaptation for semantic segmentation via class-balanced self-training. In *Proceedings of the European conference on computer vision (ECCV)*, pages 289–305, 2018.
- [45] David Berthelot, Rebecca Roelofs, Kihyuk Sohn, Nicholas Carlini, and Alex Kurakin. Adamatch: A unified approach to semi-supervised learning and domain adaptation. In *International Conference on Learning Representations (ICLR)*, 2022.
- [46] Xiaohua Zhai, Avital Oliver, Alexander Kolesnikov, and Lucas Beyer. S4l: Self-supervised semi-supervised learning. In *Proceedings of the IEEE/CVF International Conference on Computer Vision*, pages 1476–1485, 2019.
- [47] Hieu Pham and Quoc V Le. Semi-supervised learning by coaching. 2019.
- [48] Vikas Verma, Alex Lamb, Juho Kannala, Yoshua Bengio, and David Lopez-Paz. Interpolation consistency training for semi-supervised learning. In *International Joint Conference on Artificial Intelligence*, pages 3635–3641, 2019.
- [49] Yue Han, Yuhong Liu, and Zhigang Jin. Sentiment analysis via semi-supervised learning: a model based on dynamic threshold and multi-classifiers. *Neural Computing and Applications*, 32(9):5117–5129, 2020.
- [50] Zhedong Zheng and Yi Yang. Rectifying pseudo label learning via uncertainty estimation for domain adaptive semantic segmentation. *International Journal of Computer Vision*, 129(4):1106–1120, 2021.
- [51] Paola Cascante-Bonilla, Fuwen Tan, Yanjun Qi, and Vicente Ordonez. Curriculum labeling: Revisiting pseudo-labeling for semi-supervised learning. In *Proceedings of the AAAI Conference on Artificial Intelligence*, volume 35, pages 6912–6920, 2021.
- [52] Chen Wei, Kihyuk Sohn, Clayton Mellina, Alan Yuille, and Fan Yang. Crest: A class-rebalancing self-training framework for imbalanced semi-supervised learning. In *Proceedings of the IEEE/CVF Conference on Computer Vision and Pattern Recognition*, pages 10857–10866, 2021.
- [53] Jaehyung Kim, Youngbum Hur, Sejun Park, Eunho Yang, Sung Ju Hwang, and Jinwoo Shin. Distribution aligning refinery of pseudo-label for imbalanced semi-supervised learning. *Advances in Neural Information Processing Systems*, 33:14567–14579, 2020.
- [54] Hyuck Lee, Seungjae Shin, and Heeyoung Kim. Abc: Auxiliary balanced classifier for class-imbalanced semi-supervised learning. *Advances in Neural Information Processing Systems*, 34, 2021.
- [55] Yue Fan, Dengxin Dai, and Bernt Schiele. Cossl: Co-learning of representation and classifier for imbalanced semi-supervised learning. *arXiv preprint arXiv:2112.04564*, 2021.

- [56] Kuniaki Saito, Donghyun Kim, and Kate Saenko. Openmatch: Open-set semi-supervised learning with open-set consistency regularization. *Advances in Neural Information Processing Systems*, 34, 2021.
- [57] Qing Yu, Daiki Ikami, Go Irie, and Kiyoharu Aizawa. Multi-task curriculum framework for open-set semi-supervised learning. In *European Conference on Computer Vision*, pages 438–454. Springer, 2020.
- [58] Nicholas Carlini, Ulrich Erlingsson, and Nicolas Papernot. Distribution density, tails, and outliers in machine learning: Metrics and applications. *arXiv preprint arXiv:1910.13427*, 2019.
- [59] Diederik P Kingma and Jimmy Ba. Adam: A method for stochastic optimization. *arXiv preprint arXiv:1412.6980*, 2014.

A Proof of Theorem 2.1

Theorem 2.1 For a binary classification problem as mentioned above, the pseudo label Y_p has the following probability distribution:

$$\begin{aligned} P(Y_p = 1) &= \frac{1}{2} \Phi\left(\frac{\frac{\mu_2 - \mu_1}{2} - \frac{1}{\beta} \log\left(\frac{\tau}{1-\tau}\right)}{\sigma_2}\right) + \frac{1}{2} \Phi\left(\frac{\frac{\mu_1 - \mu_2}{2} - \frac{1}{\beta} \log\left(\frac{\tau}{1-\tau}\right)}{\sigma_1}\right), \\ P(Y_p = -1) &= \frac{1}{2} \Phi\left(\frac{\frac{\mu_2 - \mu_1}{2} - \frac{1}{\beta} \log\left(\frac{\tau}{1-\tau}\right)}{\sigma_1}\right) + \frac{1}{2} \Phi\left(\frac{\frac{\mu_1 - \mu_2}{2} - \frac{1}{\beta} \log\left(\frac{\tau}{1-\tau}\right)}{\sigma_2}\right), \\ P(Y_p = 0) &= 1 - P(Y_p = 1) - P(Y_p = -1), \end{aligned} \quad (15)$$

where Φ is the cumulative distribution function of a standard normal distribution. Moreover, $P(Y_p = 0) = 0$ increases as $\mu_2 - \mu_1$ gets smaller.

Proof. A sample x will be assigned pseudo label 1 if

$$\frac{1}{1 + \exp\left(-\beta\left(x - \frac{\mu_1 + \mu_2}{2}\right)\right)} > \tau,$$

which is equivalent to

$$x > \frac{\mu_1 + \mu_2}{2} + \frac{1}{\beta} \log\left(\frac{\tau}{1-\tau}\right).$$

Likewise, x will be assigned pseudo label -1 if

$$\frac{1}{1 + \exp\left(-\beta\left(x - \frac{\mu_1 + \mu_2}{2}\right)\right)} < 1 - \tau,$$

which is equivalent to

$$x < \frac{\mu_1 + \mu_2}{2} - \frac{1}{\beta} \log\left(\frac{\tau}{1-\tau}\right).$$

If we integrate over x , we arrive at the following conditional probabilities:

$$\begin{aligned} P(Y_p = 1|Y = 1) &= \Phi\left(\frac{\frac{\mu_2 - \mu_1}{2} - \frac{1}{\beta} \log\left(\frac{\tau}{1-\tau}\right)}{\sigma_2}\right), \\ P(Y_p = 1|Y = -1) &= \Phi\left(\frac{\frac{\mu_1 - \mu_2}{2} - \frac{1}{\beta} \log\left(\frac{\tau}{1-\tau}\right)}{\sigma_1}\right), \\ P(Y_p = -1|Y = -1) &= \Phi\left(\frac{\frac{\mu_2 - \mu_1}{2} - \frac{1}{\beta} \log\left(\frac{\tau}{1-\tau}\right)}{\sigma_1}\right), \\ P(Y_p = -1|Y = 1) &= \Phi\left(\frac{\frac{\mu_1 - \mu_2}{2} - \frac{1}{\beta} \log\left(\frac{\tau}{1-\tau}\right)}{\sigma_2}\right). \end{aligned}$$

Recall that $P(Y = 1) = P(Y = -1) = 0.5$, therefore

$$\begin{aligned} P(Y_p = 1) &= \frac{1}{2} \Phi\left(\frac{\frac{\mu_2 - \mu_1}{2} - \frac{1}{\beta} \log\left(\frac{\tau}{1-\tau}\right)}{\sigma_2}\right) + \frac{1}{2} \Phi\left(\frac{\frac{\mu_1 - \mu_2}{2} - \frac{1}{\beta} \log\left(\frac{\tau}{1-\tau}\right)}{\sigma_1}\right), \\ P(Y_p = -1) &= \frac{1}{2} \Phi\left(\frac{\frac{\mu_2 - \mu_1}{2} - \frac{1}{\beta} \log\left(\frac{\tau}{1-\tau}\right)}{\sigma_1}\right) + \frac{1}{2} \Phi\left(\frac{\frac{\mu_1 - \mu_2}{2} - \frac{1}{\beta} \log\left(\frac{\tau}{1-\tau}\right)}{\sigma_2}\right). \end{aligned}$$

Now, let's use z to denote $\mu_2 - \mu_1$, to show that $P(Y_p = 0)$ increases as $\mu_2 - \mu_1$ gets smaller, we only need to show $P(Y_p = -1) + P(Y_p = 1)$ gets bigger. We write $P(Y_p = -1) + P(Y_p = 1)$ as

$$P(Y_p = 1) + P(Y_p = -1) = \frac{1}{2} \Phi(a_1 z - b_1) + \frac{1}{2} \Phi(-a_1 z - b_1) + \frac{1}{2} \Phi(a_2 z - b_2) + \frac{1}{2} \Phi(-a_2 z - b_2),$$

where $a_1 = \frac{1}{2\sigma_1}$, $a_2 = \frac{1}{2\sigma_2}$, $b_1 = \frac{\log(\frac{\tau}{1-\tau})}{\beta\sigma_1}$, $b_2 = \frac{\log(\frac{\tau}{1-\tau})}{\beta\sigma_2}$ are positive constants. We further only need to show that $f(z) = \frac{1}{2} \Phi(a_1 z - b_1) + \frac{1}{2} \Phi(-a_1 z - b_1)$ is monotone increasing on $(0, \infty)$. Take the derivative of z , we have

$$f'(z) = \frac{1}{2} a_1 (\phi(a_1 z - b_1) - \phi(-a_1 z - b_1)),$$

where ϕ is the probability density function of a standard normal distribution. Since $|a_1 z - b_1| < | - a_1 z - b_1|$, we have $f'(z) > 0$, and the proof is complete. \square

B Algorithm

We present the pseudo algorithm of FreeMatch. Compared to FixMatch, each training step involves updating the global threshold and local threshold from the unlabeled data batch, and computing corresponding histograms. FreeMatchs introduce a very trivial computation budget compared to FixMatch, demonstrated also in our main paper.

Algorithm 1 FreeMatch algorithm at t -th iteration.

- 1: **Input:** Number of classes C , labeled batch $\mathcal{X} = \{(x_b, y_b) : b \in (1, 2, \dots, B)\}$, unlabeled batch $\mathcal{U} = \{u_b : b \in (1, 2, \dots, \mu B)\}$, unsupervised loss weight w_u , fairness loss weight w_f , and EMA decay λ .
 - 2: Compute \mathcal{L}_s for labeled data

$$\mathcal{L}_s = \frac{1}{B} \sum_{b=1}^B \mathcal{H}(y_b, p_m(y|\omega(x_b)))$$
 - 3: Update the global threshold

$$\tau_t = \lambda \tau_{t-1} + (1 - \lambda) \frac{1}{\mu B} \sum_{b=1}^{\mu B} \max(q_b) \quad \{q_b \text{ is an abbreviation of } p_m(y|\omega(u_b)), \text{ shape of } \tau_t: [1]\}$$
 - 4: Update the local threshold

$$\tilde{p}_t = \lambda \tilde{p}_{t-1} + (1 - \lambda) \frac{1}{\mu B} \sum_{b=1}^{\mu B} q_b \quad \{\text{Shape of } \tilde{p}_t: [C]\}$$
 - 5: Update histogram for \tilde{p}_t

$$\tilde{h}_t = \lambda \tilde{h}_{t-1} + (1 - \lambda) \text{Hist}_{\mu B}(\hat{q}_b) \quad \{\text{Shape of } \tilde{h}_t: [C]\}$$
 - 6: **for** $c = 1$ to C **do**
 - 7: $\tau_t(c) = \text{MaxNorm}(\tilde{p}_t(c)) \cdot \tau_t$ **{Calculate SAT}**
 - 8: **end for**
 - 9: Compute \mathcal{L}_u on unlabeled data

$$\mathcal{L}_u = \frac{1}{\mu B} \sum_{b=1}^{\mu B} \mathbb{1}(\max(q_b) \geq \tau_t(\arg \max(q_b))) \cdot \mathcal{H}(\hat{q}_b, Q_b)$$
 - 10: Compute expectation of probability on unlabeled data

$$\bar{p} = \frac{1}{\mu B} \sum_{b=1}^{\mu B} \mathbb{1}(\max(q_b) \geq \tau_t(\arg \max(q_b))) Q_b \quad \{Q_b \text{ is an abbr. of } p_m(y|\Omega(u_b)), \text{ shape of } \bar{p}: [C]\}$$
 - 11: Compute histogram for \bar{p}

$$\bar{h} = \text{Hist}_{\mu B} \left(\mathbb{1}(\max(q_b) \geq \tau_t(\arg \max(q_b))) \hat{Q}_b \right) \quad \{\text{Shape of } \bar{h}: [C]\}$$
 - 12: Compute \mathcal{L}_f on unlabeled data

$$\mathcal{L}_f = -\mathcal{H} \left(\text{SumNorm} \left(\frac{\tilde{p}_t}{\tilde{h}_t} \right), \text{SumNorm} \left(\frac{\bar{p}}{\bar{h}} \right) \right)$$
 - 13: **Return:** $\mathcal{L}_s + w_u \cdot \mathcal{L}_u + w_f \cdot \mathcal{L}_f$
-

C Hyperparameter setting

For reproduction, we show the detailed hyperparameter setting for FreeMatch in Table 5 and 6, for algorithm-dependent and algorithm-independent hyperparameters, respectively.

Table 5: Algorithm dependent hyperparameters.

Algorithm	FreeMatch
Unlabeled Data to Labeled Data Ratio (CIFAR-10/100, STL-10, SVHN)	7
Unlabeled Data to Labeled Data Ratio (ImageNet)	1
Loss weight w_u for all experiments	1
Loss weight w_f for CIFAR-10 (10), CIFAR-100 (400), STL-10 (40), ImageNet (100k), SVHN	0.01
Loss weight w_f for others	0.05
Thresholding EMA decay for all experiments	0.999

Table 6: Algorithm independent hyperparameters.

Dataset	CIFAR-10	CIFAR-100	STL-10	SVHN	ImageNet
Model	WRN-28-2	WRN-28-8	WRN-37-2	WRN-28-2	ResNet-50
Weight decay	5e-4	1e-3	5e-4	5e-4	3e-4
Batch size		64			128
Learning rate			0.03		
SGD momentum				0.9	
EMA decay				0.999	

Note that for ImageNet experiments, we used the same learning rate, optimizer scheme, and training iterations as other experiments, and a batch size of 128 is adopted, whereas, in FixMatch, a large batch size of 1024 and a different optimizer is used. From our experiments, we found that training ImageNet with only 2^{20} is not enough, and the model starts converging at the end of training. Longer training iterations on ImageNet will be explored in the future. Single NVIDIA V100 is used for training on CIFAR-10, CIFAR-100, SVHN and STL-10. It costs about 2 days to train on CIFAR-10 and SVHN. 10 days are needed for the training on CIFAR-100 and STL-10.

D Extensive Experiment Details and Results

We present extensive experiment details and results as complementary to the experiments in the main paper.

D.1 CIFAR-10 (10) Labeled Data

Following [6], we investigate the limitations of SSL algorithms by giving only **one labeled training sample per class**. The selected 3 labeled training sets are visualized in Figure 4, which are obtained by [6] using ordering mechanism [58].

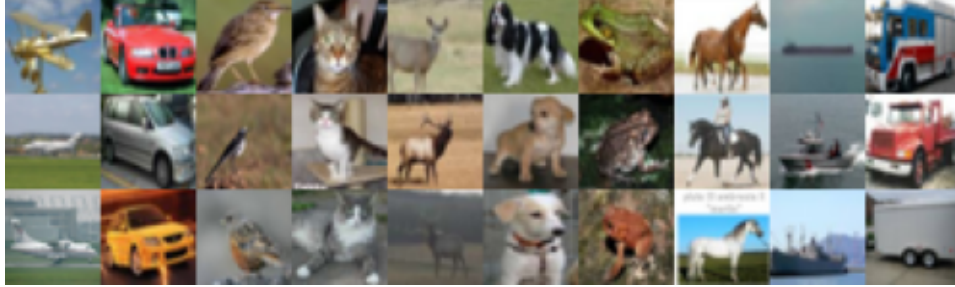


Figure 4: CIFAR-10 (10) labeled samples visualization, sorted from the most prototypical dataset (first row) to least prototypical dataset (last row).

D.2 Detailed Results

To comprehensively evaluate the performance of all methods in a classification setting, we further report the precision, recall, f1 score, and AUC (area under curve) results of CIFAR-10 with the same 10 labels, CIFAR-100 with 400 labels, SVHN with 40 labels, and STL-10 with 40 labels. As shown in Table 7 and 8, FreeMatch also has the best performance on precision, recall, F1 score, and AUC in addition to the top1 error rates reported in the main paper.

D.3 Ablation on EMA decay on CIFAR-10 (40)

We provide the ablation study on EMA decay parameter λ in Equation (7) and Equation (8). One can observe that different decay λ produces the close results on CIFAR-10 with 40 labels, indicating that FreeMatch is not sensitive to this hyper-parameter. A large λ is not encouraged since it could impede the update of global / local thresholds.

Table 7: Precision, recall, f1 score and AUC results on CIFAR-10/100.

Datasets	CIFAR-10 (10)				CIFAR-100 (400)			
	Precision	Recall	F1 Score	AUC	Precision	Recall	F1 Score	AUC
UDA	0.5304	0.5121	0.4754	0.8258	0.5813	0.5484	0.5087	0.9475
FixMatch	0.6436	0.6622	0.6110	0.8934	0.5574	0.5430	0.4946	0.9363
Dash	0.6409	0.5410	0.4955	0.8458	0.5833	0.5649	0.5215	0.9456
MPL	0.6286	0.6857	0.6178	0.7993	0.5799	0.5606	0.5193	0.9316
FlexMatch	0.6769	0.6861	0.6780	0.9126	0.6135	0.6193	0.6107	0.9675
FreeMatch	0.8619	0.8593	0.8523	0.9843	0.6243	0.6261	0.6137	0.9692

Table 8: Precision, recall, f1 score and AUC results on SVHN and STL-10.

Datasets	SVHN (40)				STL-10 (40)			
	Precision	Recall	F1 Score	AUC	Precision	Recall	F1 Score	AUC
UDA	0.9783	0.9777	0.9780	0.9977	0.6385	0.5319	0.4765	0.8581
FixMatch	0.9731	0.9706	0.9716	0.9962	0.6590	0.5830	0.5405	0.8862
Dash	0.9782	0.9778	0.9780	0.9978	0.8117	0.6020	0.5448	0.8827
MPL	0.9564	0.9513	0.9512	0.9844	0.6191	0.5740	0.4999	0.8529
FlexMatch	0.9566	0.9691	0.9625	0.9975	0.6403	0.6755	0.6518	0.9249
FreeMatch	0.9783	0.9800	0.9791	0.9979	0.8489	0.8439	0.8354	0.9792

Table 9: Error rates of different thresholding EMA decay.

Thresholding EMA decay	CIFAR-10 (40)
0.9	4.94 ± 0.06
0.99	4.92 ± 0.08
0.999	4.90 ± 0.04
0.9999	5.03 ± 0.07

Table 10: Error rates (%) on CIFAR-10-LT and CIFAR-100-LT of 3 different random seeds. The best number is in bold.

Dataset	CIFAR-10-LT		CIFAR-100-LT	
Imbalance γ	50	150	20	100
FixMatch [6]	18.5 ± 0.48	31.2 ± 1.08	49.1 ± 0.62	62.5 ± 0.36
FlexMatch [21]	17.8 ± 0.24	29.5 ± 0.47	48.9 ± 0.71	62.7 ± 0.08
FreeMatch	17.7 ± 0.33	28.8 ± 0.64	48.4 ± 0.91	62.5 ± 0.23
FixMatch w/ ABC [54]	14.0 ± 0.22	22.3 ± 1.08	46.6 ± 0.69	58.3 ± 0.41
FlexMatch w/ ABC	14.2 ± 0.34	23.1 ± 0.70	46.2 ± 0.47	58.9 ± 0.51
FreeMatch w/ ABC	13.9 ± 0.03	22.3 ± 0.26	45.6 ± 0.76	58.9 ± 0.55

D.4 Ablation of Imbalanced SSL

To further prove the effectiveness of FreeMatch, We evaluate FreeMatch on the imbalanced SSL setting [53, 52, 54, 55], where the labeled and the unlabeled data are both imbalanced. We conduct experiments on CIFAR-10-LT and CIFAR-100-LT with different imbalance ratios. The imbalance ratio used on CIFAR datasets is defined as $\gamma = N_{max}/N_{min}$ where N_{max} is the number of samples on the head (frequent) class and N_{min} the tail (rare). Note that the number of samples for class k is computed as $N_k = N_{max} \gamma^{-\frac{k-1}{C-1}}$, where C is the number of classes. Following [54, 55], we set $N_{max} = 1500$ for CIFAR-10 and $N_{max} = 150$ for CIFAR-100, and the number of unlabeled data is twice as many for each class. We use a WRN-28-2 [35] as the backbone. We use Adam [59] as the optimizer. The initial learning rate is 0.002 with a cosine learning rate decay schedule as $\eta = \eta_0 \cos(\frac{7\pi k}{16K})$, where η_0 is the initial learning rate, $k(K)$ is the current (total) training step and we set $K = 2.5 \times 10^5$ for all datasets. The batch size of labeled and unlabeled data is 64 and 128, respectively. Weight decay is set as 4e-5. Each experiment is run on three different data splits, and we report the average of the best error rates.

The results are summarized in Table 10. Compared with other standard SSL methods, FreeMatch achieves the best performance across all settings. Especially on CIFAR-10 at imbalance ratio 150, FreeMatch outperforms the second best by 2.4%. Moreover, when plugged in the other imbalanced SSL method [54], FreeMatch still attains the best performance in most of the settings.

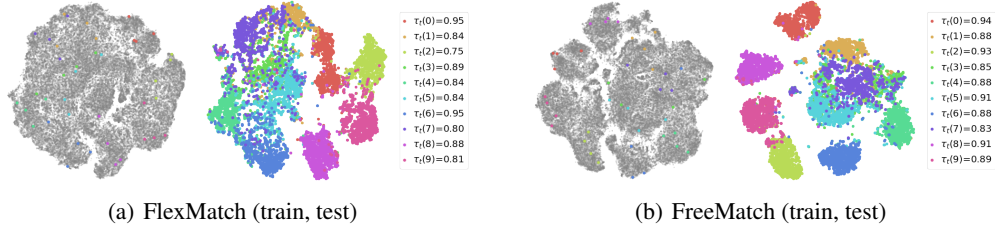


Figure 5: T-SNE visualization of FlexMatch and FreeMatch features on STL-10 (40). Unlabeled data is indicated by gray color. Local threshold $\tau_t(c)$ for each class is shown on the legend.

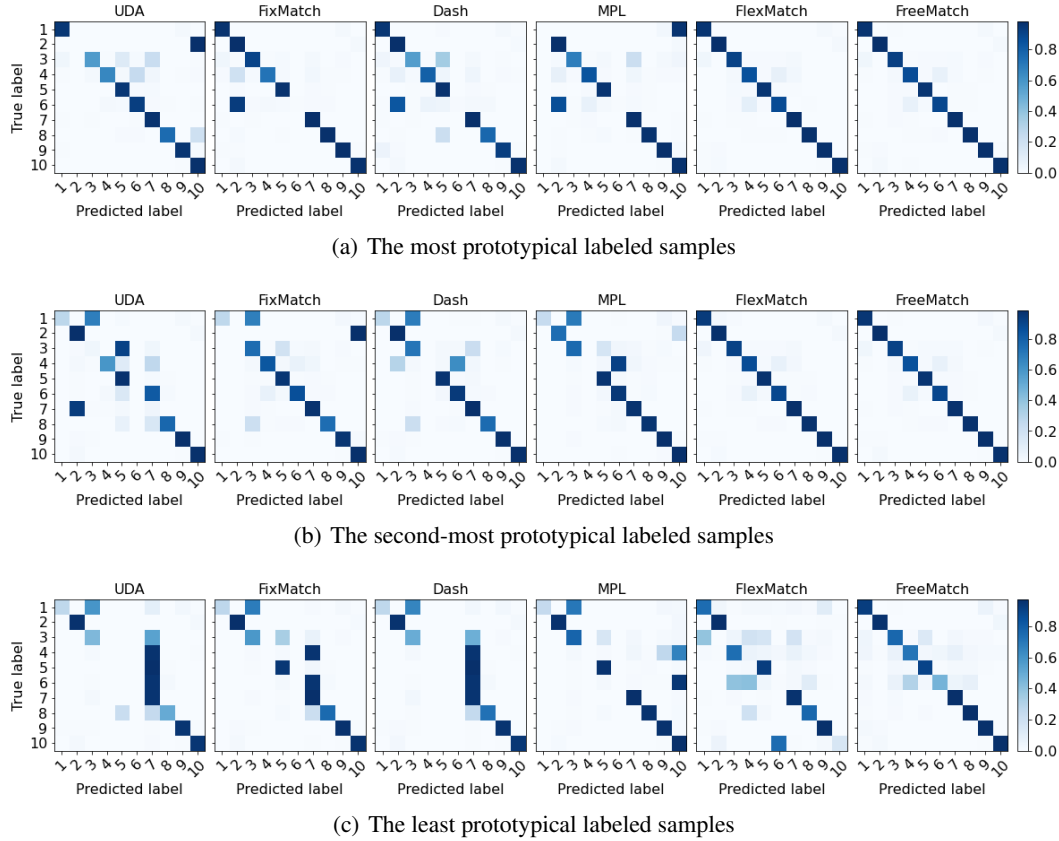


Figure 6: Confusion matrix on the test set of CIFAR-10 (10). Rows correspond to the rows in Figure 4. Columns correspond to different SSL methods.

D.5 T-SNE Visualization on STL-10 (40)

We plot the T-SNE visualization of the features on STL-10 with 40 labels from FlexMatch [21] and FreeMatch. FreeMatch shows better feature space than FlexMatch with less confusing clusters.

D.6 CIFAR-10 (10) Confusion Matrix

We plot the confusion matrix of FreeMatch and other SSL methods on CIFAR-10 (10) in Figure 6. It is worth noting that even with the least prototypical labeled data in our setting, FreeMatch still gets good results while other SSL methods fail to separate the unlabeled data into different clusters, showing inconsistency with the low-density assumption in SSL.